DALTON
FULL PAPER

Structural and dynamic properties of calixarene bimetallic complexes: solution *versus* solid-state structure of dinuclear complexes of Eu^{III} and Lu^{III} with substituted calix[8]arenes †

Jean-Claude G. Bünzli,*[a] Frédéric Ihringer,[a] Pascal Dumy,[b] Cédric Sager[b] and Robin D. Rogers[c]

[a] *Institute of Inorganic and Analytical Chemistry, University of Lausanne, BCH 1402, CH-1015 Lausanne, Switzerland*
[b] *Institute of Organic Chemistry, University of Lausanne, BCH, CH-1015 Lausanne, Switzerland*
[c] *Department of Chemistry, The University of Alabama, Tuscaloosa, Alabama 35487-0336, USA*

The solid state (Ln = Eu) and solution (Ln = Lu) structure of the dinuclear complexes $[Ln_2L(dmf)_5]\cdot x$solv, where L is the hexaanion of *p*-nitrocalix[8]arene (n-H_8L) or *p-tert*-butylcalix[8]arene (b-H_8L) and dmf = dimethylformamide, have been analysed and compared. The neutral $[Eu_2(n\text{-}H_2L)(dmf)_5]$ species displays C_2 symmetry with the axis perpendicular to the Eu–Eu internuclear axis. The europium(III) ions are separated by 3.810(1) Å and are surrounded by eight O atoms, with six Eu–O distances in the range 2.2–2.4 Å (two phenoxides, two μ-phenoxides and two dmf) while the remaining Eu–O bond lengths are much longer (2.7–2.9 Å, one phenol and one μ-dmf). The geometry of the dinuclear assembly is comparable to that observed for $[Eu_2(b\text{-}H_2L)(dmf)_5]\cdot 4$dmf, both ligands adopting a two-bladed propeller conformation. The solution structure of $[Lu_2L(dmf)_5]$, L = b-H_2L^{6-} and n-H_2L^{6-}, has been investigated by ^{1}H NMR spectroscopy in [$^2H_7$]dmf. The dinuclear complexes retain a two-fold symmetry element and the ligand conformation is identical for both edifices and very close to the solid-state conformation. An intramolecular racemisation process has been evidenced and characterised at 294 K: $k = 7.0 \pm 0.7\ s^{-1}$, $\Delta G^{\ddagger} = 67.1 \pm 0.4$ kJ mol^{-1} (b-H_8L) and $k = 1.1 \pm 0.1\ s^{-1}$, $\Delta G^{\ddagger} = 71.6 \pm 0.4$ kJ mol^{-1} (n-H_8L).

The past ten years have seen sustained progress in the complexation and supramolecular chemistry of the trivalent lanthanide ions. This renewed interest is mainly due to fast developing biomedical applications[1] of rare-earth-metal-containing systems, for instance in nuclear magnetic imaging,[2] cancer therapy,[3,4] specific cleavage of DNA and RNA,[5–7] fluoroimmunoassays and luminescent labelling of biomolecules.[8] In reference to the latter uses, a great deal of attention has been devoted to the design of lanthanide-based (mainly Eu^{III}, Tb^{III} and Sm^{III}) luminescent probes,[8,9] which require very specific, and sometimes somewhat contradictory, properties: *e.g.* facile population of the ligand $^1\pi\pi^*$ and $^3\pi\pi^*$ states to ensure efficient subsequent energy transfer onto the metal ion, and protection of the lanthanoid(III) excited states against non-radiative deexcitation processes through high-energy vibrations or mixing of the 4f states with either the ligand states or, in the case of Eu^{III}, with the ligand-to-metal charge-transfer (LMCT) state.[10] To meet this challenge, chemists have applied different strategies based on the use of polyaminocarboxylic chelates,[8,11] of self-assembly processes[12,13] or preorganised macrocyclic receptors.[14–16] Among the latter, calixarenes emerged as easy-to-synthesize and versatile hosts[17–19] which are helpful in the design of lanthanide-containing luminescent stains.[20–24] Whereas most of the work with lanthanide ions has concentrated on calix[4]arenes,‡[20–23,25–27] we have launched a programme aiming at untangling the photophysical and structural properties of lanthanide complexes with calix[8]arenes,‡ which were shown to encapsulate two lanthanide ions.[28,29] Such supramolecular assemblies are model molecules to test lanthanide-to-lanthanide energy-transfer processes and can also provide two luminescent stains in one edifice, *i.e.* when two different lanthanoid(III) ions are encapsulated.

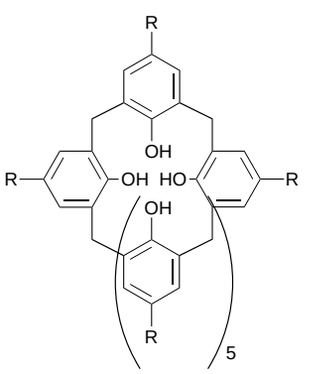

b-H_8L R = $C(CH_3)_3$
n-H_8L R = NO_2

Our investigation first focused on dinuclear complexes with *p-tert*-butylcalix[8]arene (b-H_8L).[30,31] While b-H_8L acts as a good sensitizer for Tb^{III}, the replacement of the *p-tert*-butyl groups by electron-attracting nitro groups (n-H_8L) shifts the $^1\pi\pi^*$ and $^3\pi\pi^*$ states to lower energy and the LMCT state to higher energy, resulting in a better sensitisation of Eu^{III}, but prevents any ligand-to-Tb^{III} energy-transfer process.[32] Upper-rim substitution of calix[8]arene therefore provides a good handle to tune the photophysical properties of their lanthanide-containing complexes. In this paper we present the solid-state structure of $[Eu_2(n\text{-}H_2L)(dmf)_5]\cdot 3dmf\cdot H_2O$ **1** (dmf = dimethylformamide) and compare it to the structure of the corresponding complex with *p-tert*-butylcalix[8]arene **2**.[28] Reports on the solution structure of f-block metal-ion complexes with calixarenes are scarce despite the great interest in them for solvent

† *Supplementary data available*: table of angles and figures of the coordination polyhedron of Eu^{III} in $[Eu_2(n\text{-}H_2L)(dmf)_5]\cdot 3dmf\cdot H_2O$; ^{1}H NMR spectra of n-H_8L, b-H_8L, $[Lu(b\text{-}H_6L)(NO_3)(dmf)_4]$, $[Lu(b\text{-}H_2L)(dmf)_5]$ and $[Lu_2(n\text{-}H_2L)(dmf)_5]$; DQF-COSY and ROESY ^{1}H NMR spectra of $[Lu_2(n\text{-}H_2L)(dmf)_5]$ and $[Lu_2(b\text{-}H_2L)(dmf)_5]$. For direct electronic access see http://www.rsc.org/suppdata/dt/1998/497/, otherwise available from BLDSC (No. SUP 57324, 9 pp.) or the RSC library. See Instructions for Authors, 1998, Issue 1 (http://www.rsc.org/dalton).

‡ IUPAC names: calix[4]arene = $1^2,3^2,5^2,7^2$-tetrahydroxy-1,3,5,7(1,3)-tetrabenzenacyclooctaphane; calix[8]arene = $1^2,3^2,5^2,7^2,9^2,11^2,13^2,15^2$-octahydroxy-1,3,5,7,9,11,13,15(1,3)-octabenzenacyclohexadecaphane.

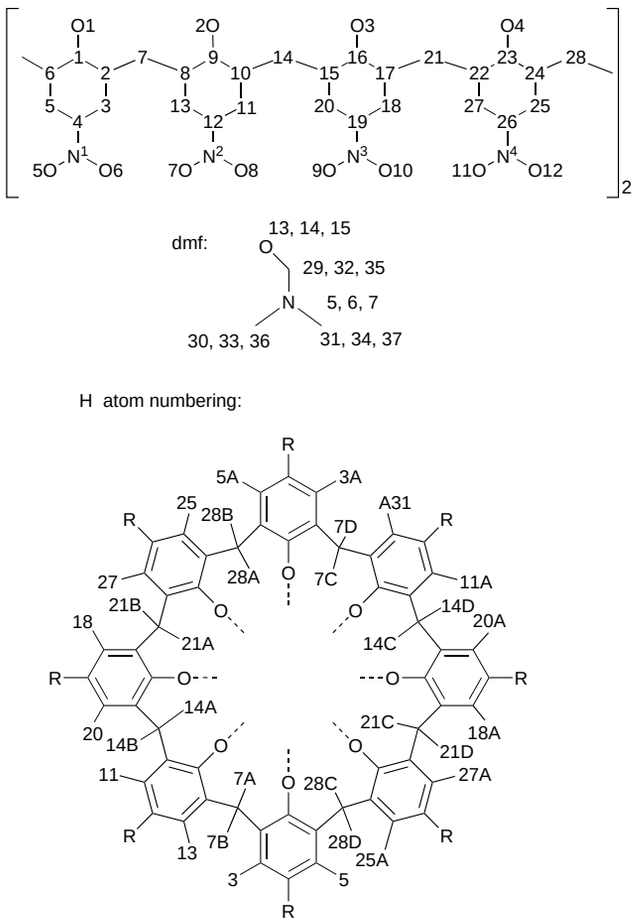

Fig. 1 Top: atom numbering scheme for $[Eu_2(n\text{-}H_2L)(dmf)_5]\cdot 3dmf\cdot H_2O$ **1**. In the text equivalent atoms are designated by capital letters and their coordinates are obtained by the symmetry transformation $-x+\frac{7}{4}$, $-y+\frac{3}{4}$, z. Bottom: H atom numbering scheme used to interpret ^1H NMR spectra

extraction.[33,34] We have therefore undertaken an NMR study to resolve the structure of the diamagnetic lutetium(III) complexes with both b-H_8L and n-H_8L with the aim of determining the ligand conformation in solution and discussing the influence of the *para* substituent on the structural properties of the dinuclear edifices. Furthermore, a dynamic process between two distinct conformations of the macrocycles could be evidenced and quantitatively characterised for both dinuclear lutetium(III) complexes.

Results and Discussion

Solid-state structure of complex 1

Details of the X-ray experimental conditions, cell data, structure solution and refinement are given in the Experimental section while the atom-numbering scheme is shown in Fig. 1. The asymmetric unit consists of 16 neutral dinuclear complexes $[Eu_2(n\text{-}H_2L)(dmf)_5]$ with C_2 symmetry (Fig. 2). The two europium(III) ions are surrounded by eight O atoms from four phenoxides (two of them bridging the two metal ions), three dmf molecules (one of which is bridging), and one phenol group. Six Eu–O distances are in the expected range 2.215(8)–2.399(8) Å while the remaining two Eu–O contacts are much longer [2.704(7), 2.919(2) Å] and arise respectively from interaction with the bridging dmf molecule and probably with the undissociated phenol group (the H atom could not be located but solvent water molecules are within hydrogen-bonding distance for the phenol). Analysis of the Eu–O bond distances with reference to those found in **2** (Table 1) indicates shorter Eu–O1 and longer Eu–O2 and Eu–O3 bonds in **1**, resulting in

Table 1 The Eu–Eu and Eu–O distances (Å) in $[Eu_2(n\text{-}H_2L)(dmf)_5]\cdot 3dmf\cdot H_2O$ **1** and $[Eu_2(b\text{-}H_2L)(dmf)_5]\cdot 4dmf$ **2** (α phase)[28]

Bond[a]	**1**	**2**[b]
Eu · · · EuA	3.810(2)	3.692(1)
Eu–O1 (phenoxide)	2.266(7)	2.386(5)
Eu–O3 (phenoxide)	2.215(8)	2.168(4)
Eu–O4 (μ-phenoxide)	2.384(7)	2.351(5)
Eu–O4A (μ-phenoxide)	2.399(8)	2.365(5)
Eu–O13 (dmf)	2.375(7)	2.379(5)
Eu–O14 (dmf)	2.384(7)	2.373(5)
Mean Eu–O (6 distances)	2.34(8)	2.34(8)
Eu–O2 (phenol)	2.92(1)	2.771(7)
Eu–O15 (μ-dmf)	2.704(7)	2.657(5)
Mean Eu–O (8 distances)	2.46(24)	2.43(19)

[a] Atoms labelled A are generated by symmetry operations. [b] Averages of two bond lengths (the Eu atoms lie in slightly different environments in complex **2**).

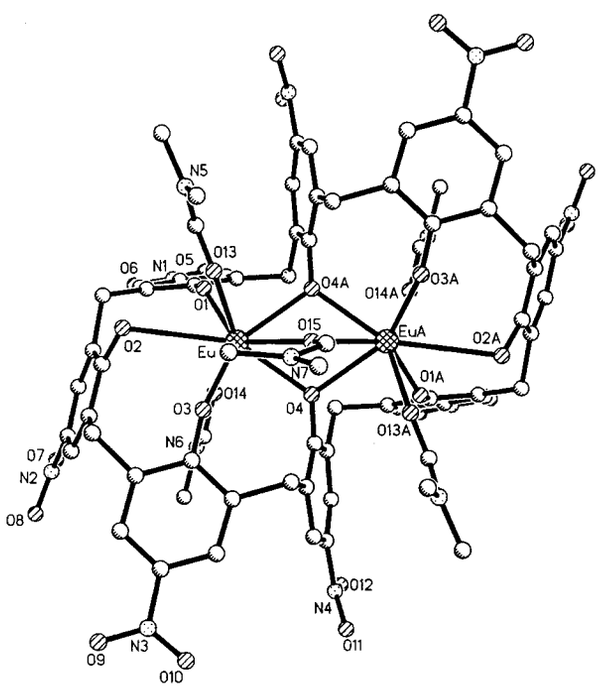

Fig. 2 An ORTEP[35] view of the neutral complex $[Eu_2(n\text{-}H_2L)(dmf)_5]$. The two-fold axis goes through O15 and is perpendicular to the internuclear Eu–Eu axis

metal ions less centred in the calixarene cavity than in **2**, henceforth the longer Eu · · · Eu distance, 3.810(2) Å, as compared to 3.692(1) Å in **2**.[28] The co-ordination polyhedra of the europium(III) ions in **1** and **2** may be regarded as distorted bicapped trigonal prisms,[24,30] O2 and O15 acting as the capping atoms (Fig. F1, Table S1 of SUP 57324). Luminescence spectra confirm this interpretation since emission lines from the europium $^5D_0$ level have a pattern close to the one measured for a species with pseudo-trigonal symmetry.[30,32] It is noteworthy that the mean Eu–O distance calculated with the six 'fully bonding' O atoms is identical in **1** and **2**. The corresponding effective ionic radius, estimated according to Shannon's definition[36] with $r_O = 1.31$ Å, amounts to 1.03 Å and is larger than the literature value of 0.95 Å for six-co-ordination.[37] On the other hand, the radii calculated by taking into account the eight contacts are larger (1.15 and 1.12 Å for **1** and **2**, respectively) than the literature value for eight-co-ordination (1.07 Å[37]), and correspond to the radius quoted for nine-co-ordination (1.12 Å[37]).

The ligand conformation (Fig. 3) is very different from that of the free molecule[38] and can be viewed as if the calix[8]arene would consist of two calix[4]arenes in the cone conformation and placed side by side in a 'transoid' configuration, as exem-

Table 2 Selected dihedral angles (°) between phenolic planes in $[Eu_2L(dmf)_5]$, L = n-H_2L **1** or b-H_2L **2**, as calculated with the PACHA program.[39] For the plane numbering see Fig. 2

Angle	1–2	2–3	3–4	4–1A	1–1A	2–2A	3–3A	4–4A
1	60	73	75	85	168	148	147	153
2*	58	65	74	82	165	135	167	147

* Average value calculated for planes corresponding to those defined in complex **1** (**2** does not display C_2 symmetry).

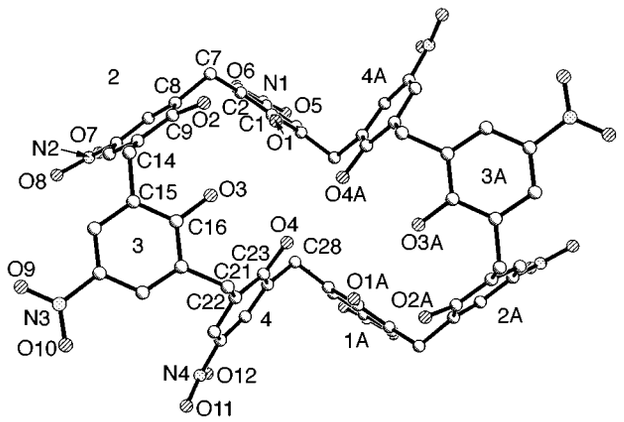

Fig. 3 An ORTEP view of the ligand conformation in complex **1**, showing the numbering of the phenol groups

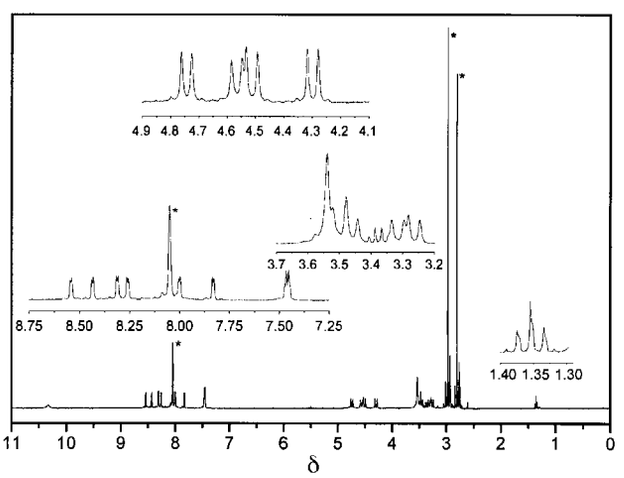

Fig. 4 Proton NMR spectrum (360 MHz) of 10^{-2} M $[Lu_2(n\text{-}H_2L)(dmf)_5]$ in $[^2H_7]$dmf at room temperature. Stars denotes resonances from bonded dmf

plified by the dihedral angle between rings 4 and 1A (Fig. 3) close to 90°. The conformation is analogous to the two-bladed propeller conformation described for **2**[28] (Table 2) and it brings the O atoms closer to each other than in the free molecule conformation, so that the ligand cavity matches better the ionic radius of the metal ions, allowing the co-ordination of two lanthanoid(III) ions through bridging of phenoxide groups. In $[(UO_2)_2(b\text{-}H_4L)(OH)]^-$ none of the phenol or phenoxide groups is bridging, the two U atoms being linked by a hydroxide ion, and the conformation of the ligand is close to the free calixarene conformation.[40,41]

Solution structure of $[Lu_2(n\text{-}H_2L)(dmf)_5]$ 3

Diamagnetic lutetium was chosen for determination of solution structures by NMR spectroscopy since its complexes produce sharp NMR lines. The one-dimensional ^{1}H NMR spectrum of a 10^{-2} M solution of complex **3** in $[^2H_7]$dmf (Fig. 4) displays three groups of signals arising from the ligand: (i) eight doublets between δ 7.46 and 8.53 from the 16 aromatic protons, (ii) two groups of four doublets in the range δ 3.24–4.77 assigned to the methylene protons, and (iii) one broad singlet at δ 10.3 corresponding to the two hydroxyl protons. In addition, signals from free water (singlet at δ 3.54, one molecule per molecule of **3**) and from co-ordinated dmf (distinct from the partially deuteriated dmf at δ 2.76, 2.94 and 8.05) are observed; integration of the dmf signals at δ 2.81 and 2.98 yields 4.7 dmf molecules per molecule of **3**, in line with the chemical formulation of the dinuclear complex and indicating that almost no exchange with $[^2H_7]$dmf occurs. Finally, a triplet (δ 1.36) and a quartet (δ 3.38) are assigned to triethylammonium, either free or complexed by the ligand. Indeed, Gutsche *et al.*[42] have shown that the interaction between calixarenes and amines involves a two-step process, *viz.* proton transfer from the calixarene to the amine followed by the association of the two ions formed; they have shown that the amine resonances then undergo a downfield shift from δ 0.96 and 2.43 (neat) to 1.18 and 3.10 for the complex with *p*-allylcalix[4]arene in dmf (δ 1.30 and 3.25 in dmf in presence of an excess of trifluoroacetic acid).[42] The association constants connected with these steps have been estimated by several authors for various bases and calix[*n*]arenes ($n = 4$, 6 or 8).[42–44] In our case a solution of the europium complex **1** displays the same signals as a solution of **3**, indicating that the protonated base does not lie in the vicinity of the metal ion. Moreover, integration of the NMR signals points to the presence of one complexed triethylamine molecule per 10 molecules of complex. Such a small amount of base remains undetected by elemental and X-ray analyses of the isolated complexes. The ^{1}H NMR spectrum shows little variation with temperature, between 47.2 and −22.5 °C, except for a downfield shift of the water resonance and a broadening of the signals resulting in the pairwise coalescence of the signals associated with the aromatic protons.

At this stage it is important to identify clearly the species in solution. Besançon[44] has shown the complexation process leading to the formation of the dinuclear complexes with b-H_8L to consist of three steps: formation of a 1:1 complex (similar to the one isolated by Harrowfield *et al.*[45]) and transformation into the 2:1 complex going through an observable reaction intermediate having a 1:1 Eu^{III} to ligand ratio; the estimated log K_{21} is 5.[44] Taking this figure into account, we calculate our solution to contain less than 5% (9.5% if we take log $K_{21} = 4$) of the mononuclear species, which therefore would not be observable in the NMR spectrum. This is confirmed by comparing the spectra of the free calixarene, of the 1:1 species and of the dinuclear complex under similar experimental conditions (Fig. F3, SUP 57324). The latter does not display identifiable signals from the first two species. Therefore, we are confident that the spectrum of Fig. 4 is characteristic of the 2:1 species and that the observed triethylammonium cation does not influence the metal-ion environment, nor the overall ligand conformation.

The observation of 17 signals for 34 protons implies a two-fold symmetry element for $[Lu_2(n\text{-}H_2L)(dmf)_5]$, C_2, C_s or *i*. To get further insight into the solution structure we have performed DQF-COSY (double quantum filtered correlation spectroscopy) (Fig. F4, SUP 57324) and ROESY (rotating frame Overhauser enhancement spectroscopy) (see Fig. 5) experiments. Complete relative assignment of the protons was achieved as follows (see Fig. 1 for the numbering scheme). (i) The doublet at δ 4.75 was assigned to H7A; the DQF-COSY experiment points to the signal at δ 3.26 arising from the geminal H7B proton. (ii) Dipolar interactions are evidenced between H7B and the two aromatic protons H3 and H13 by ROESY correlation peaks (Fig. F5, SUP 57324). (iii) Designation of the aromatic protons bound to the same phenol ring follows from the DQF-COSY data, *e.g.* H5 couples with H3 and H13 with H11. (iv) Protons H5 and H11 display nuclear Overhauser effects with H28D and H14B, and so on. (v) Nuclear Overhauser effects observed between aromatic protons of adjacent phenol rings confirm this assignment (Table 3),

Table 3 Proton NMR shifts (ppm) and coupling constants (Hz) for $[Lu_2L(dmf)_5]$ in $[^2H_7]$dmf at room temperature; L = n-H_2L^{6-} (10^{-2} M, **3**) or b-H_2L^{6-} (7×10^{-3} M, **4**). See Fig. 1 for the numbering scheme

Compound		OH	3	5	11	13	18	20	25	27	7A	7B	14A	14B	21A	21B	28A	28B
3	δ	10.33	8.53	8.31	7.82	7.99	8.26	8.42	7.47	7.46	4.75	3.26	4.58	3.45	4.30	3.31	4.52	3.49
	J	—	3.0	2.9	3.0	3.0	3.0	3.1	2.9	2.8	12.9	13.1	13.0	13.1	13.9	14.3	14.4	14.8
4	δ	11.80	7.34	7.21	7.26	6.63	7.05	7.00	7.14	6.97	4.92	2.90	4.99	2.92	3.82	3.14	4.76	2.94
	J	—	—	—	—	—	—	—	—	—	12.1	12.2	14.3	13.6	12.6	12.6	11.5	11.5

Compound		*tert*-butyl				H_2O	NEt_3		dmf		
3	δ	—	—	—	—	3.54	3.38	1.36	8.05	2.98	2.81
	J	—	—	—	—	—	7.4	7.4	—	—	—
4	δ	1.35	1.29	1.17	1.09	3.51	2.46	0.97	8.05	2.98	2.81
	J	—	—	—	—	—	7.2	7.2	—	—	—

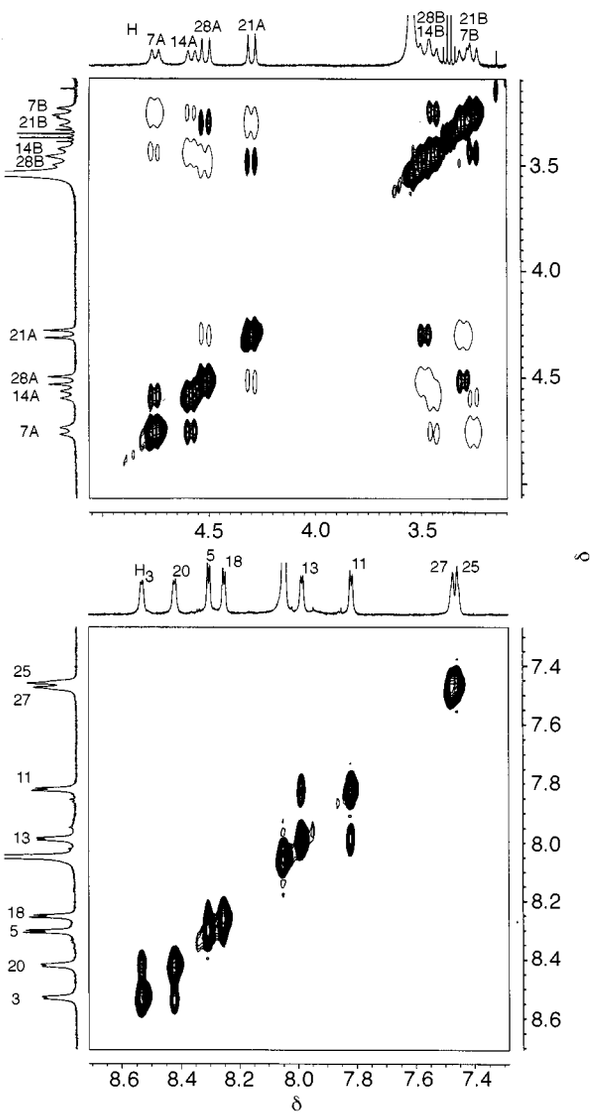

Fig. 5 The ROESY ^{1}H NMR spectra (400 MHz) of 10^{-2} M $[Lu_2(n\text{-}H_2L)(dmf)_5]$ in $[^2H_7]$dmf at room temperature. Top: methylene protons. Bottom: aromatic protons. One-contour peaks represent nuclear Overhauser effects while the other peaks arise from exchange contributions

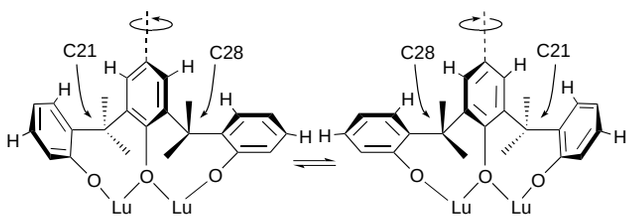

Scheme 1 Conformational exchange mechanism in complex **3** as unravelled by ROESY experiments

which is not unambiguous: for instance H3 could be H5, but this is without consequence for the overall symmetry of the molecule. A symmetry plane is now ruled out, but we cannot decide formally between C_2 and *i*. In the solid state the series of bimetallic complexes with b-H_2L (Ln = La, Eu, Tm or Lu) exhibits similar structure, as far as the ligand conformation is concerned.[46] Therefore, we infer from our X-ray diffraction (Ln = Eu) and NMR (Ln = Lu) study that the solution structure of complex **3** probably displays an averaged C_2 symmetry. Dissociation of bonded dmf molecules does not occur, as exemplified by the observation of only one $^5D_0 \longleftarrow {}^7F_0$ transition in the absorption spectrum.[32]

The ROESY data point to an exchange process which interconverts the chemical environment of pairs of protons, without changing the overall ligand conformation: (i) H7A and H14A, H7B and H14B, H21A and H28B, H21B and H28A and (ii) H3 and H20, H5 and H18, H13 and H11, H27 and H25. Examination of the crystal structure of complex **1** reveals two distinct conformations for the methylene groups, with protons pointing inside (one group) or outside (three groups) the ligand cavity. The interconversion between the chemical environment of H21A and H28B, and of H21B and H28A, is only possible between two methylene groups pointing respectively inside and outside the cavity and the two-dimensional NMR data indicate they are attached to the same phenol ring. The only candidates are protons on the bridging phenolates which rotate around an axis going through the O atom and the C atom in *para* position. The associated mechanism is shown in Scheme 1 where C21 and C28 exchange chemical environments. In fact this corresponds to an intramolecular racemisation process. We note that **1** crystallises as a racemic mixture and that due to the process evidenced from the NMR data a synthesis with a chiral base would probably not lead to an optically active complex as found for the dinuclear titanium complex with b-H_8L.[47,48]

Solution structure of $[Lu_2(b\text{-}H_2L)(dmf)_5]$ 4 and dynamic study of complexes 3 and 4

In previous work we have concluded, from the number of observed signals, that the one-dimensional NMR spectrum of $[Y_2(b\text{-}H_2L)(dmf)_5]$ is consistent with C_2 symmetry.[24] To complete the comparison between the solid-state and solution structure of the complexes with n-H_8L and b-H_8L, we have thoroughly investigated a 7×10^{-3} M solution of **4** in $[^2H_7]$dmf. Its one-dimensional NMR spectrum (Fig. 6) displays four groups of signals arising from the ligand and corresponding to aromatic (eight singlets), methylenic (eight doublets), methylic (four singlets) and alcoholic protons (one singlet). In addition,

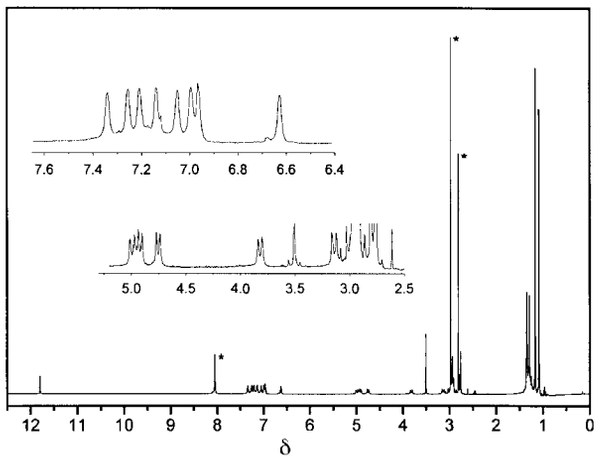

Fig. 6 Proton NMR spectrum (360 MHz) of 7×10^{-3} M [Lu_2-(b-H_2L)(dmf)$_5$] in [$^2H_7$]dmf at room temperature. Stars denote resonances from bonded dmf

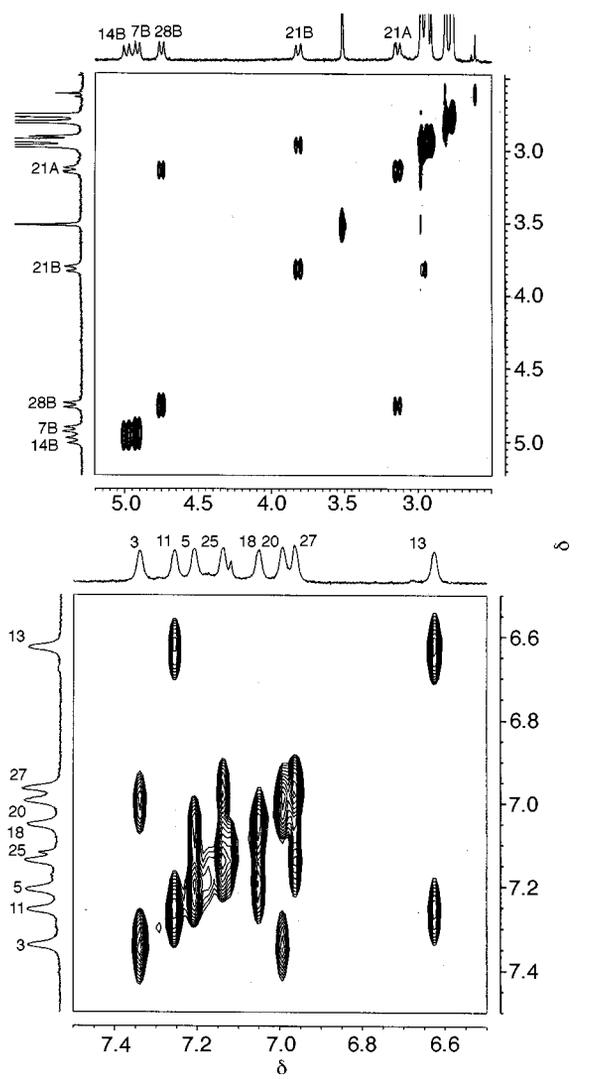

Fig. 7 The NOESY ^{1}H NMR spectra (400 MHz) of 7×10^{-3} M [Lu_2(b-H_2L)(dmf)$_5$] in [$^2H_7$]dmf at room temperature, recorded with 100 ms mixing time. Top: methylene protons. Bottom: aromatic protons

we find signals from bonded dmf (5.7 molecules per molecule of **4**), water (1.5 molecule per molecule of **4**) and free triethylamine (δ 0.97 and 2.46; 1 molecule per 15 molecules of **4**). This spectrum is consistent with a dinuclear species (*cf.* Fig. F3, SUP 57324) having a two-fold symmetry element. The DQF-COSY and ROESY experiments (Figs. F6 and F7, SUP 57324) allowed us to establish the assignments reported in Table 3 and to conclude that **3** and **4** have very similar solution structures. Moreover, **4** also undergoes a racemisation process and the signals from the methyl groups confirm the proposed mechanism (Scheme 1). The peaks at δ 1.09 and 1.17 are sharp (full width at half height, f.w.h.h. = 1.5 Hz), the corresponding methyl groups do not exchange and are attached to aromatic rings the *meta*-protons of which are exchanging (H11, H13 and H25, H27). On the other hand, the methyl groups generating peaks at δ 1.29 and 1.35 (f.w.h.h. = 5 Hz) belong to the aromatic rings with *m*-protons H3, H5 and H18, H20 and are undergoing an exchange process. The latter prevented us from assigning the two signals to methyl groups attached to specific phenolic rings.

Nuclear Overhauser enhancement spectroscopy (NOESY) experiments (Fig. 7) helped us to quantify the intramolecular exchange process between the two chiral conformations of the complexes: comparison with the ROESY spectra indicates that all the correlation peaks in the NOESY spectra correspond to two exchange processes, an intermolecular one between the water molecules and the hydroxyl groups of the phenol rings and an intramolecular one involving the ligand. The rate constant k of the latter racemisation process has been evaluated using formulae (1) and (2):[49] where I_{AA} and I_{AB} represent the

$$\frac{I_{AA}}{I_{AB}} = \frac{1 + e^{-2k\tau_m}}{1 - e^{-2k\tau_m}} \quad (1)$$

$$k = \text{arcth}(I_{AB}/I_{AA})/\tau_m \quad (2)$$

areas of the diagonal and correlation peaks, respectively, τ_m is the mixing time (100 ms under the conditions used for recording the spectra of Fig. 7) and arcth is the arc of the hyperbolic tangent. The formulae are valid provided the exchange takes place between two equally populated sites ($k_{AB} = k_{BA} = k$), and provided the spin–lattice relaxation rates are identical ($R_1^A = R_1^B$), as well as the transverse relaxation times ($T_2^A = T_2^B$). These conditions are fulfilled for an intramolecular process and analysis of the I_{AA}/I_{AB} ratios for the three couples (H11, H13), (H5, H18) and (H28A, H21B) leads for [Lu_2(b-H_2L)(dmf)$_5$] to k(294 K) = 7.0 ± 0.7 s^{-1} and, using Eyring's formula, $\Delta G^{\ddagger}$ = 67.1 ± 0.4 kJ mol^{-1}. For [Lu_2(n-H_2L)(dmf)$_5$] the estimation is more difficult, the NOESY correlation peaks being weak, and only one pair of protons (H11, H13) could be used to estimate the kinetic parameters: k(294 K) = 1.1 ± 0.1 s^{-1} and $\Delta G^{\ddagger}$ = 71.6 ± 0.4 kJ mol^{-1}. We assign the slower exchange in **3**, compared to **4**, to a larger interaction between the *para* substituents and the solvent. To our knowledge, these kinetic data are the first ones reported for bimetallic edifices with calix[8]arenes, while other two-dimensional NMR studies have focused on free calixarenes. For instance, Janssen *et al.*[50] have measured $\Delta G^{\ddagger}$ = 61 kJ mol^{-1} for the interconversion between the undulated conformation of free b-H_8L and its mirror image in benzene.

Conclusion

The series of complexes [Ln_2(b-H_2L)(dmf)$_5$] (Ln = La, Pr, Eu or Lu) have similar solid-state structures, with the ligand adopting a two-bladed propeller conformation and allowing the binding of two metal ions at short intermetallic distances (3.6–3.8 Å).[29] The data reported in this paper demonstrate that this arrangement is maintained in solution and, furthermore, both in the solid state and in solution when the bulky *para-tert*-butyl groups are substituted by nitro groups. These supramolecular assemblies retain electroneutrality in solution, which could be of interest in magnetic resonance imaging, a field in which efforts are made to replace the presently used anionic species by neutral complexes.[2] Moreover, complexation by the lanthanide ions does not completely rigidify the structure, with the ligand continuing to undergo a pseudo-rotation of the phenol rings,

resulting in a fast racemisation process, evidenced for the first time in the case of a metal complex with calixarene, and in an overall structure retaining a two-fold symmetry element. In subsequent papers we shall deal with the kinetics of formation of lanthanide-containing bimetallic complexes with calix[8]-arenes.

Experimental

Synthesis

Ligands b-H_8L and n-H_8L were synthesized and purified according to known literature procedures.[30,32] The complexes of Eu^{III} and Lu^{III} were obtained from dmf (Fluka, *puriss*) solutions in the presence of an excess of triethylamine (Fluka, *puriss*), using the general procedure described by Furphy *et al.*[28] Yellow crystals of $[Eu_2(n\text{-}H_2L)(dmf)_5]\cdot 3dmf\cdot H_2O$ **1** suitable for X-ray diffraction study were grown from a dmf solution into which methanol was slowly diffused during 30 d. The Lu-containing complexes gave satisfactory elemental analyses for $[Lu_2L_2(dmf)_5]\cdot x$dmf with $x = 2$ for L = n-H_2L^{6-} (**3**) and $x = 0$ for L = b-H_2L^{6-} (**4**). The complexes are efflorescent and may display variable solvation,[32] they were pumped under vacuum before preparing the solutions for NMR measurements.

NMR measurements

Control spectra were recorded with a Bruker AM-360 (360 MHz) spectrometer, two-dimensional spectra on a Bruker ARX (400 MHz) spectrometer. Chemical shifts were determined using the residual formylic protons of [$^2H_7$]dmf (Armar, 99.5 atom% D: ^{1}H, δ 8.05). Two-dimensional spectra were acquired using 2048 × 512 matrices over a 4500 Hz sweep width in both dimensions. Quadrature detection was achieved through the TPPI (time proportional phase increments) procedure.[51] Scalar connectivities were obtained from DFQ-COSY experiments[52] and dipolar couplings from conventional NOESY[53] and ROESY[54] sequences with mixing times between 50 and 200 ms. The spin-lock period of the ROESY sequences was applied by coherent continuous-wave irradiation at $\gamma B_2/2\pi = 2$ kHz, where γ is the gyromagnetic ratio and B_2 the magnetic field. Experimental data were handled with the UXNMR program from Bruker; the standard sinebell squared routine was used for apodisation with a shift range of 60–90° and zero filling was applied to both dimensions to obtain 2K × 2K square matrices with real data points. Assignment of the resonances was confirmed by HMQC (heteronuclear multiple quantum correlation) experiments[55] and the relative error on the Gibbs free energy was calculated according to expression (3).[56]

$$\Delta\Delta G^{\ddagger}/\Delta G^{\ddagger} = \left\{ \left[\frac{\Delta T}{T} \left(\ln \frac{k_B T}{hk} \right) + 1 \right]^2 + \left(\frac{\Delta k}{k} \right)^2 \right\}^{\frac{1}{2}} \Big/ \ln(k_B T/hk) \quad (3)$$

X-Ray crystallography

A single crystal of complex **1** was mounted on a fibre and transferred to the goniometer. The crystal was cooled to −100 °C during data collection by using a stream of cold nitrogen gas. The space group was determined to be *Fddd* from the systematic absences. A summary of data collection and structure refinement is given in Table 4. The europium complex resides around a crystallographic two-fold axis which necessitates that the bridging dmf molecule be disordered. The disorder of this molecule was resolved so that O15 resides on the two-fold axis and N7, C35, C36, and C37 are present at 50% occupancy fractionally disordered about the C_2 axis. Several nitro groups exhibited high thermal motion but only one could be resolved into a disorder model: two alternative positions were resolved for O11 and O12 and these atoms were included at 50% occupancy. The methyl H atoms of the four dmf molecules bonded in a monodentate way to the europium ions were included as rigid groups with $B = 1.2U_{eq}$(C). Refinement of non-H atoms was carried out with anisotropic thermal parameters.

Table 4 Summary of crystal data, data collection, structure solution and refinements details for $[Eu_2(n\text{-}H_2L)(dmf)_5]\cdot 3dmf\cdot H_2O$

Formula	$C_{80}H_{92}Eu_2N_{16}O_{33}$
M	2109.62
Colour, habit	Yellow parallelepiped
Crystal size/mm	0.18 × 0.20 × 0.60
Crystal system	Orthorhombic
Space group	*Fddd*
a/Å	27.1031(4)
b/Å	34.9926(1)
c/Å	43.0044(5)
U/Å^3	40785.7(8)
Z	16
F(000)	17 184
D_c/g cm^{-3}	1.374
μ/mm^{-1}	1.301
Unit-cell reflections (θ range/°)	7433 (1.06–27.86)
hkl Ranges	−33 to 35, −36 to 45, −47 to 55
Reflections measured	55 357
Unique reflections	11 913 (R_{int} = 0.1092)
Reflections with $I > 2\sigma$	5283
Absorption correction	SADABS[57]
Extinction coefficient	0.000 039(6)
Range of relative transmission factors	0.97 to 0.72
Refinement method	Full-matrix least squares on F^2, no restraint
Solution method	Direct methods
Hydrogen atom treatment	Riding, $B = 1.2U_{eq}$(C)
No. variables	570
Goodness of fit on F^2	1.056
Final *R*1, *wR*2 indices ($I \geqslant 2\sigma$)	0.0983, 0.2521
(all data)	0.2032, 0.3322
Density range in final map/e Å^{-3}	1.782 and −0.689

Data collection on a Siemens SMART instrument with CCD area detector and graphite-monochromatised Mo-Kα radiation (λ = 0.7107 Å). Computing was done with SHELXTL.[58]

Chemical analysis revealed a formulation including three solvent dmf and one water molecule per dinuclear complex. This would require 1.5 dmf and $\frac{1}{2}$ H_2O molecules in the asymmetric unit. Resolution of the unco-ordinated solvent and water molecules was problematic. Two partially (25% each) occupied positions were located for the water molecule. These make sense because they are within hydrogen-bonding distance of O2. Several diffuse peaks were observed in the unit cell which could arise from dmf molecules; however, it was not possible to resolve these. Contributions from these dmf and H_2O molecules were therefore not included in the final refinement. Possible locations of these molecules are in the eight cavities displayed by the unit cell (Fig. F2, SUP 57324), of approximate dimensions 11 × 6 × 27 Å and having a surface mostly comprised of O atoms from the nitro groups (the molar volume of a dmf molecule is 81 Å^3).

CCDC reference number 186/798.

See http://www.rsc.org/suppdata/dt/1998/497/ for crystallographic files in .cif format.

Acknowledgements

This research is supported through grants from the Swiss National Science Foundation. We thank Dr. Loïc Charbonnière for his help in interpreting NMR spectra. R. D. R. is grateful to the US National Science Foundation for support related to the purchase of the CCD-equipped diffractometer (Grant CHE-9626144).

References

1 C. H. Evans, *Biochemistry of the Lanthanides*, Plenum, New York, 1990.
2 R. B. Lauffer, in *MRI Clinical Magnetic Resonance Imaging*, eds. R. E. Edelman, M. B. Zlatkin and J. R. Hesselink, W. B. Saunders Co., Philadelphia, 1996, vol. 1, ch. 5.
3 J. L. Sessler, V. Kral, M. C. Hoehner, K. O. A. Chin and R. M. Davila, *Pure Appl. Chem.*, 1996, **68**, 1291.
4 D. Parker and J. A. Williams, *J. Chem. Soc.*, *Dalton Trans.*, 1996, 3613.
5 J. Hall, D. Hüsken and R. Häner, *Nucl. Acids Res.*, 1996, **24**, 3522.
6 K. G. Ragunathan and H. J. Schneider, *Angew. Chem.*, *Int. Ed. Engl.*, 1996, **35**, 1219.
7 M. Komiyama, J. Kamitani, J. Sumaoka and H. Asanuma, *Chem. Lett.*, 1996, 869.
8 I. Hemmilä, T. Stahlberg and P. Mottram, *Bioanalytical Applications of Labelling Technologies*, Wallac Oy, Turku, 1995.
9 *Lanthanide Probes in Life*, *Chemical and Earth Sciences*: *Theory and Practice*, eds. J.-C. G. Bünzli and G. R. Choppin, Elsevier, Amsterdam, 1989
10 J.-C. G. Bünzli, S. Petoud, C. Piguet and F. Renaud, *J. Alloys Compd.*, 1997, **249**, 14.
11 M. Latva, H. Takalo, K. Simberg and J. Kankare, *J. Chem. Soc.*, *Perkin Trans. 2*, 1995, 995.
12 M. Latva, P. Makinen, S. Kulmala and K. Haapakka, *J. Chem. Soc.*, *Faraday Trans.*, 1996, **92**, 3321.
13 C. Piguet, J.-C. G. Bünzli, G. Bernardinelli, G. Hopfgartner, S. Petoud and O. Schaad, *J. Am. Chem. Soc.*, 1996, **118**, 6681.
14 N. Sabbatini, M. Guardigli, I. Manet, R. Ungaro, A. Casnati, R. Ziessel, G. Ulrich, Z. Asfari and J. M. Lehn, *Pure Appl. Chem.*, 1995, **67**, 135.
15 V. Alexander, *Chem. Rev.*, 1995, **95**, 273.
16 J.-C. G. Bünzli, P. Froidevaux and C. Piguet, *New J. Chem.*, 1995, **19**, 661.
17 *Calixarenes*: *A Versatile Class of Macrocyclic Compounds*, eds. J. Vicens and V. Böhmer, Kluwer, Dordrecht, 1991.
18 V. Böhmer, *Angew. Chem.*, *Int. Ed. Engl.*, 1995, **34**, 713.
19 M. Takeshita and S. Shinkai, *Bull. Chem. Soc. Jpn.*, 1995, **68**, 1088.
20 A. Casnati, C. Fischer, M. Guardigli, A. Isernia, I. Manet, N. Sabbatini and R. Ungaro, *J. Chem. Soc.*, *Perkin Trans. 2*, 1996, 395.
21 D. M. Rudkevich, W. Verboom, E. Vandertol, C. J. Van Staveren, F. M. Kaspersen, J. W. Verhoeven and D. N. Reinhoudt, *J. Chem. Soc.*, *Perkin Trans. 2*, 1995, 131.
22 F. J. Steemers, W. Verboom, D. N. Reinhoudt, E. B. Vandertol and J. W. Verhoeven, *J. Am. Chem. Soc.*, 1995, **117**, 9408.
23 N. Sato and S. Shinkai, *J. Chem. Soc.*, *Perkin Trans. 2*, 1993, 621.
24 J.-C. G. Bünzli and J. M. Harrowfield, in *Calixarenes*: *a Versatile Class of Macrocyclic Compounds*, eds. J. Vicens and V. Böhmer, Kluwer, Dordrecht, 1991, 211.
25 M. F. Hazenkamp, G. Blasse, N. Sabbatini and R. Ungaro, *Inorg. Chim. Acta*, 1990, **172**, 93.
26 S. Pappalardo, F. Bottino, L. Giunta, M. Pietraszkiewicz and J. Karpiuk, *J. Incl. Phenom. Mol. Recognit. Chem.*, 1991, **10**, 387.
27 E. M. Georgiev, J. Clymire, G. L. McPherson and D. M. Roundhill, *Inorg. Chim. Acta*, 1994, **227**, 293.
28 B. M. Furphy, J. M. Harrowfield, D. L. Kepert, B. W. Skelton, A. H. White and F. R. Wilner, *Inorg. Chem.*, 1987, **26**, 4231.
29 J. M. Harrowfield, M. I. Ogden and A. H. White, *Aust. J. Chem.*, 1991, **44**, 1237.
30 J.-C. G. Bünzli, P. Froidevaux and J. M. Harrowfield, *Inorg. Chem.*, 1993, **32**, 3306.
31 P. Froidevaux and J.-C. G. Bünzli, *J. Phys. Chem.*, 1994, **98**, 532.
32 J.-C. G. Bünzli and F. Ihringer, *Inorg. Chim. Acta*, 1996, **246**, 195.
33 F. Arnaud-Neu, V. Böhmer, J. F. Dozol, C. Gruttner, R. A. Jakobi, D. Kraft, O. Mauprivez, H. Rouquette, M.-J. Schwing-Weill, N. Simon and W. Vogt, *J. Chem. Soc.*, *Perkin Trans. 2*, 1996, 1175.
34 F. Arnaud-Neu, S. Cremin, S. Harris, M. A. McKervey, M.-J. Schwing-Weill, P. Schwinte and A. Walker, *J. Chem. Soc.*, *Dalton Trans.*, 1997, 329.
35 C. K. Johnson, ORTEP, Report ORNL-5138, Oak Ridge National Laboratory, Oak Ridge, TN, 1976.
36 R. D. Shannon, *Acta Crystallogr.*, *Sect. A*, 1976, **32**, 751.
37 G. R. Choppin, in *Lanthanide Probes in Life*, *Chemical and Earth Sciences. Theory and Practice*, eds. J.-C. G. Bünzli and G. R. Choppin, Elsevier, Amsterdam, 1989, ch. 1, pp. 1–41.
38 C. D. Gutsche, A. E. Gutsche and A. I. Karaulov, *J. Incl. Phenom. Mol. Recognit. Chem.*, 1985, **3**, 447.
39 M. Henry, Program PACHA, Partial Atomic Charge Analysis, Université Louis Pasteur, Strasbourg, 1993.
40 P. Thuery, N. Keller, M. Lance, J. D. Vigner and M. Nierlich, *New J. Chem.*, 1995, **19**, 619.
41 P. Thuery, N. Keller, M. Lance, J. D. Vigner and M. Nierlich, *Acta Crystallogr.*, *Sect. C*, 1995, **51**, 1570.
42 C. D. Gutsche, M. Iqbal and A. Iftikhar, *J. Am. Chem. Soc.*, 1987, **109**, 4314.
43 A. F. Danil De Namor, P. M. Blackett, M. T. G. Pardo, D. A. P. Tanaka, F. J. S. Velarde and M. C. Cabaleiro, *Pure Appl. Chem.*, 1993, **65**, 415.
44 F. Besançon, Ph.D. Dissertation, University of Lausanne, 1996.
45 J. M. Harrowfield, M. I. Ogden, W. R. Richmond and A. H. White, *J. Chem. Soc.*, *Dalton Trans.*, 1991, 2153.
46 J. M. Harrowfield, M. I. Ogden and A. H. White, *Aust. J. Chem.*, 1991, **44**, 1249.
47 G. E. Hofmeister, F. E. Hahn and S. F. Pedersen, *J. Am. Chem. Soc.*, 1989, **111**, 2318.
48 G. E. Hofmeister, E. Alvarado, J. A. Leary, D. I. Yoon and S. F. Pedersen, *J. Am. Chem. Soc.*, 1990, **112**, 8843.
49 A. Molins, P. M. Nieto, C. Sanchez, P. Prados, J. de Mendoza and M. Pons, *J. Org. Chem.*, 1992, **57**, 6924.
50 R. G. Janssen, J. P. M. van Duynhoven, W. Verboom, G. J. van Hummel, S. Harkema and D. N. Reinhoudt, *J. Am. Chem. Soc.*, 1996, **118**, 3666.
51 G. Drobny, A. Pines, S. Sinton, D. Weritekamp and D. Wemmer, *Faraday Symp. Chem. Soc.*, 1978, **13**, 48.
52 V. Piantini, O. W. Sorensen and R. R. Ernst, *J. Am. Chem. Soc.*, 1982, **104**, 6800.
53 J. Jeener, B. H. Meier, P. Bachmann and R. R. Ernst, *J. Chem. Phys.*, 1979, **71**, 4546.
54 A. A. Bothner-By, R. L. Stephen, J. Lee, C. D. Warren and R. W. Jeanloz, *J. Am. Chem. Soc.*, 1997, **106**, 811.
55 A. Bax, R. Griffey and B. L. Hawkins, *J. Am. Chem. Soc.*, 1986, **108**, 2093.
56 J. Sandström, *Dynamic NMR Spectroscopy*, Academic Press, London, 1982.
57 G. M. Sheldrick, SADABS, Program for semiempirical absorption correction of area detector data, University of Göttingen, 1996.
58 G. M. Sheldrick, SHELXTL, version 5, Siemens Analytical Instruments, Madison, WI, 1996.

Received 25*th September* 1997; *Paper* 7/06933B